
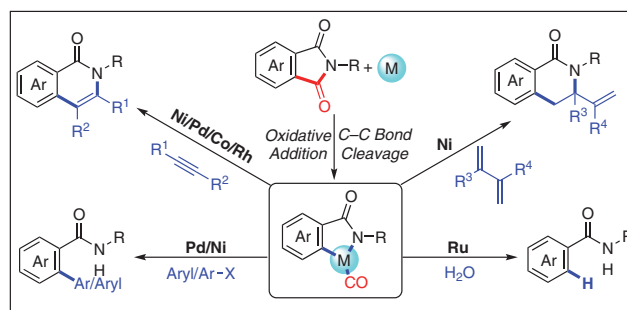


# Transition-Metal-Catalyzed Decarbonylative Functionalization of Phthalimides

Ying-Ying Liu<sup>a,b</sup>Shao-Han Sun<sup>a,b</sup>Xiang-Ting Min<sup>\*a</sup>Boshun Wan<sup>a</sup>Qing-An Chen<sup>\*a</sup> 

<sup>a</sup> Dalian Institute of Chemical Physics, Chinese Academy of Sciences, 457 Zhongshan Road, Dalian, 116023, P. R. of China  
minxiangting@dicp.ac.cn  
qachen@dicp.ac.cn  
http://www.lbcsc.dicp.ac.cn

<sup>b</sup> University of Chinese Academy of Sciences, Beijing, 100049, P. R. of China



Received: 28.12.2021

Accepted after revision: 26.01.2022

Published online: 26.01.2022

DOI: 10.1055/a-1751-1929; Art ID: ss-2021-r0793-sr

**Abstract** Phthalimide derivatives are prevalent in a wide array of biologically important molecules, including drugs, fungicides, and anticancer molecules. Thus, catalytic methods that directly edit the phthalimide moiety, in particular, decarbonylation and derivatization, could be strategically valuable for the modification of existing phthalimide molecular scaffolds. In recent years, considerable efforts have been devoted to emulating the transition-metal-catalyzed phthalimide decarbonylative reaction. A set of elegant strategies, including decarbonylative addition reactions with alkynes, alkenes, and benzynes, decarbonylative polymerization, alkylation, arylation, and protodecarbonylation, have been demonstrated. This review aims to highlight these advances and discusses the mechanism issues, to further expand application and promote developments in this field.

- 1 Introduction
- 2 Decarbonylative Addition Reaction with Alkynes
- 3 Decarbonylative Addition Reaction with Alkenes
- 4 Decarbonylative Addition Reaction with Benzyne
- 5 Decarbonylative Polymerization
- 6 Decarbonylative Alkylation
- 7 Decarbonylative Arylation
- 8 Protodecarbonylation
- 9 Conclusion and Outlook

**Key words** decarbonylation reactions, phthalimides, amides, C–N bond activation, isoquinolones, alkynes, alkenes

## 1 Introduction

As the most well-known and studied phthalimide derivative, thalidomide has been used as a sedative-hypnotic since 1958. Although it was banned in 1962 as a consequence of its unexpected dominant teratogenicity, the bioactivities of thalidomide toward other diseases have been discovered gradually.<sup>1</sup> So far, phthalimide derivatives have shown some pharmaceutical applications and been used as scaffolds for drugs such as amphotalide,<sup>2</sup> otezla,<sup>3</sup> pomalyst,<sup>4</sup>



**Ying-Ying Liu** was born in Hubei Province, China, in 1998. She obtained her B.S. degree from Dalian University of Technology (DUT) in 2020. Currently, she works in the group of Prof. Qing-An Chen at Dalian Institute of Chemical Physics (DICP) as a graduate student. Her research focuses on catalytic transformations of alkynes and alkenes.

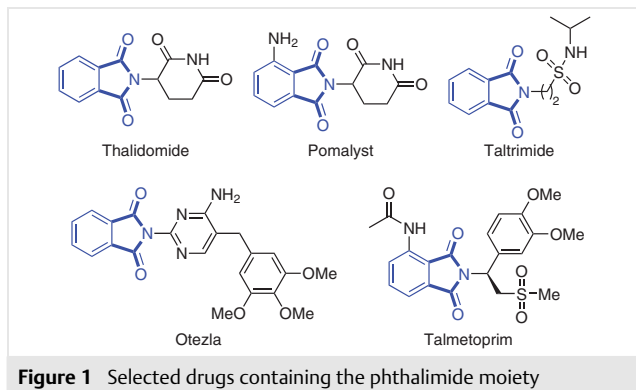
**Shao-Han Sun** was born in Liaoning Province, China, in 1998. He obtained his B.S. degree from Huazhong University of Science and Technology in 2020. Currently, he works in the group of Prof. Qing-An Chen at DICP as a graduate student. His research focuses on catalytic transformations of alkynes and alkenes.

**Xiang-Ting Min** was born in Shandong Province, China, in 1992. He obtained his B.S. degree from Liaocheng University in 2015 and M.S. degree from DUT in 2018, under the supervision of Prof. Jianhui Liu. He then obtained his PhD from DICP in 2021, under the supervision of Prof. Boshun Wan and Prof. Qing-An Chen. His research focuses on catalytic transformations of alkynes and alkenes and C–C/C–H bond activation.

**Boshun Wan** is a full professor at DICP. His research interests include asymmetric catalysis, catalytic heterocycle synthesis, and energetic material synthesis. He received his B.S. degree from Nanjing Normal University in 1985 and PhD from DICP in 1998. He then joined DICP as a group leader. He has been a visiting professor at Northwestern University, USA.

**Qing-An Chen** was born in 1984 in Fujian Province, China. He received a B.S. degree from the University of Science and Technology of China in 2007 and earned his PhD from DICP in 2012 under the supervision of Prof. Yong-Gui Zhou. He then worked with Prof. Vy M. Dong at the University of California Irvine (USA) as a postdoctoral fellow from 2012 to 2015. Later he joined Prof. Martin Oestreich's group at the Technische Universität Berlin (Germany) as an Alexander von Humboldt Fellow. In 2017, he began his independent career at DICP, where he is currently a professor of chemistry. His research interests include asymmetric catalysis and organometallic chemistry.

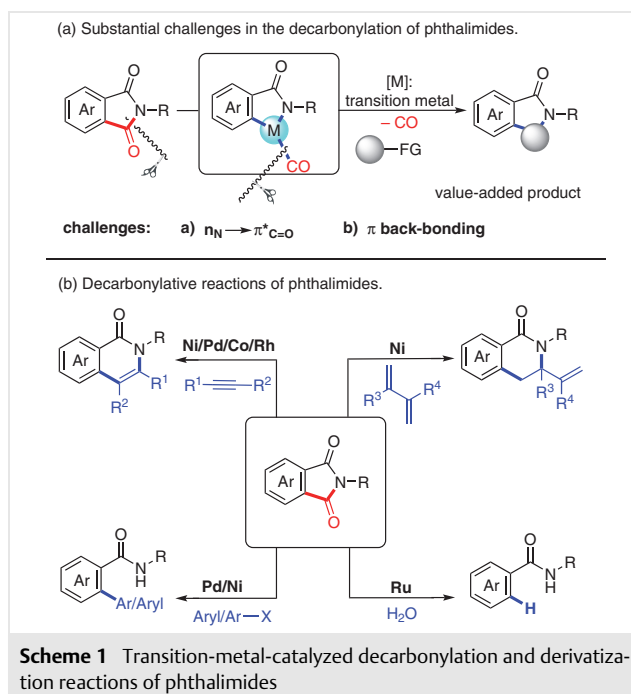
taltrimide,<sup>5</sup> and talmetoprim<sup>6</sup> (Figure 1). Recently, phthalimide derivatives have been used as anticancer and antitumor drugs.<sup>7</sup> The prevalence of the phthalimide scaffold in pharmaceutical and fine chemical libraries has attracted extensive interest for site-selective derivatization to access new chemicals.<sup>8</sup>



Recently, transition-metal-catalyzed decarbonylation of amides or imides has garnered significant attention because it provides a new and creative synthetic strategy using carbonyl groups as ‘traceless handles’ for amide modification.<sup>9</sup> Thus, a decarbonylative functionalization reaction of phthalimides that directly edits the phthalimide moiety could be strategically valuable for the modification of existing phthalimide molecular scaffolds. In addition, phthalimides are electronically activated amides, in which  $N_{lp}$  delocalization ( $lp$  = lone pair) is possible through the amide bond as well as the aromatic ring.<sup>10</sup>

Theoretically, there are substantial challenges for the transition-metal-catalyzed decarbonylation of phthalimides. In general, they can be summarized as two aspects: (1) As a result of the strong  $n_N \rightarrow \pi^*_{C=O}$  conjugation, direct oxidative addition of the C–N bond with transition metals has always been a challenging topic.<sup>11</sup> (2) Because of the  $\pi$ -backbonding between the CO  $p^*$  orbitals and metal center d orbitals, breaking the metal–carbonyl bond is another challenge (Scheme 1).<sup>12,13</sup>

Historically, the field of Ni-catalyzed decarbonylative addition reactions of phthalimides with alkynes was launched by the Matsubara and Kurahashi group in 2008.<sup>14</sup> They also found that 1,3-dienes<sup>15</sup> and trimethylsilyl-substituted alkynes<sup>16</sup> were suitable substrates in Ni-catalyzed decarbonylative addition reactions with phthalimides. Apart from nickel catalysts, in the past decade, Pd<sup>17</sup>, Rh<sup>18</sup>, Co<sup>19</sup>, and Ru<sup>20</sup> have been developed for use in decarbonylation and derivatization reactions of phthalimides by our group and others. In some cases, the reactions are not only facilitated by the typical reactivity of phthalimides but also enabled by a directing group on the phthalimides. At present, transition-metal-catalyzed decarbonylation of phthalimid-



es represents an attractive method for the construction of a wide variety of polysubstituted amides.

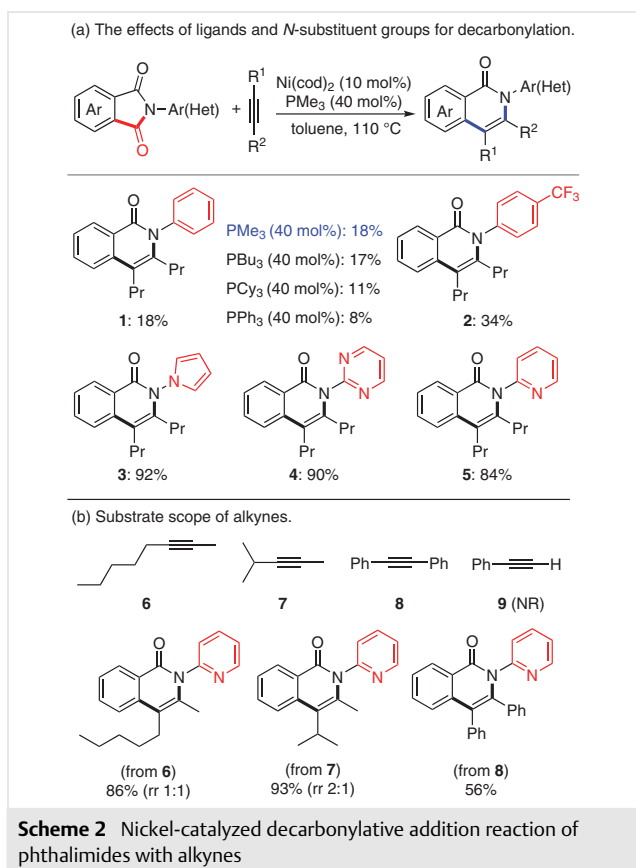
In this Short Review, we mainly focus on recent advances in transition-metal-catalyzed decarbonylation and derivatization reactions of phthalimides. For a better discussion and understanding, this review is arranged by the type of addition or coupling components. Throughout the review, we give special attention to the reaction mechanism to reveal versatile achievements, especially in the decarbonylation step. Furthermore, we summarize the unique synthetic advantages of the developed decarbonylation reactions, which will definitely further expand their application and promote development in this field.

## 2 Decarbonylative Addition Reaction with Alkynes

### 2.1 Nickel Catalysis

In 2008, the Kurahashi and Matsubara group reported the first example of a nickel-catalyzed decarbonylative addition reaction of phthalimides with alkynes (Scheme 2).<sup>14</sup> With the oxidative addition of nickel into the N–C(O) bond of phthalimide, decarbonylation and alkyne insertion steps subsequently took place. Overall, the nickel-catalyzed intermolecular carboamidation of alkynes had been developed in a single step by forming the C–C and C–N bonds simultaneously. In fact, direct oxidative addition of an Ni(0) catalyst into a C–N bond generated the active species, which was the main challenge. The authors postulated that in-

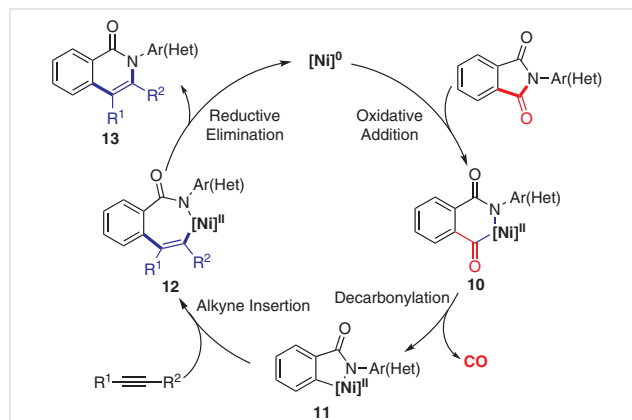
creasing the nucleophilicity of the nickel catalyst and the electrophilicity of the carbonyl group of the imide would conquer the obstacles. In particular, electron-donating  $\text{PMe}_3$  ligands promoted the transformation and gave the desired product in 18% isolated yield. In addition, trace or lower amounts of **1** were obtained by using  $\text{PBu}_3$ ,  $\text{PCy}_3$ , and  $\text{PPh}_3$  in place of  $\text{PMe}_3$  (17%, 11%, and 8% yields, respectively) (Scheme 2a). Furthermore, the reaction of *N*-phenylphthalimides **2** possessing an electron-withdrawing group afforded the correspondingly product in 34% yield. Subsequently, they found that electron-deficient *N*-arylphthalimides **3–5** could react with alkynes efficiently and gave the desired products in approximately 90% yields (Scheme 2a).



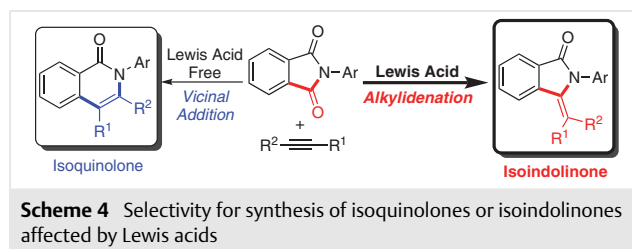
Interestingly, different types of alkynes exhibited various reactivities. Unsymmetrical dialkyl alkynes **6** and **7** gave products in excellent yields but with low regioselectivities (1:1 to 2:1). Symmetrical diphenyl alkyne **8** reacted slowly and gave the corresponding isoquinolone in moderate yield. Terminal phenylacetylene **9** failed to participate in the reaction, presumably because of rapid oligomerization (Scheme 2b).

A plausible mechanism for the nickel-catalyzed decarbonylative addition reaction of phthalimides with alkynes is depicted in Scheme 3. Firstly, with the help of the electron-rich phosphine ligand,  $\text{Ni}(0)$  undergoes oxidative addi-

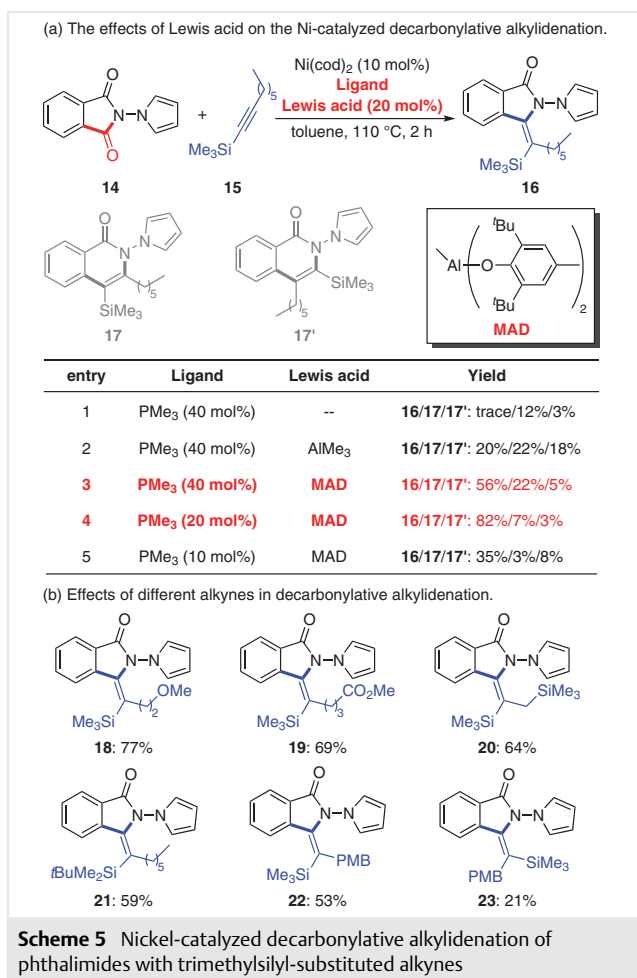
tion to give the nickelacycle **10**. Subsequent decarbonylation and insertion of alkynes to the C–Ni bond leads to the seven-membered nickelacycle complex **12**, which undergoes reductive elimination to give desired product **13** with regeneration of the initial  $\text{Ni}(0)$  complex.<sup>20</sup>



In subsequent research, a distinct decarbonylative addition reaction was reported by the Kurahashi and Matsubara group in 2010.<sup>15</sup> An unprecedented nickel and Lewis acid cocatalyzed decarbonylative reaction pattern occurred in this reaction. It provided isoindolinone products instead of isoquinolones when the Lewis acid methylaluminum bis(2,6-di-*tert*-butyl-4-methylphenoxy) (MAD) was added as a cocatalyst (Scheme 4).

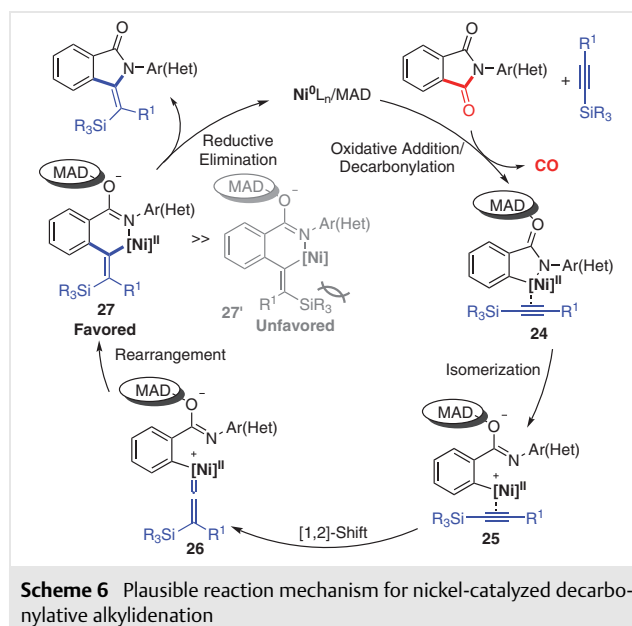


For this decarbonylative alkylidene reaction, the Lewis acids and ligands played major roles in selective regulation. These effects are summarized in Scheme 5a. According to the previous vicinal addition conditions, when phthalimide **14** and alkyne **15** were treated in the presence of  $\text{Ni}(\text{cod})_2$  (10 mol%) and  $\text{PMe}_3$  (40 mol%) for 2 h, only a trace amount of isoindolinone **16** was observed (entry 1). However, **16** could be obtained in 20% yield in the presence of 20 mol% trimethylaluminum (entry 2). The addition of a catalytic amount of MAD, a sterically bulky and monomeric homogeneous Lewis acid, gave the best results and afforded **16** in 56% yield (entry 3). Finally, **16** was obtained in 82% yield by decreasing the loading of ligands to 20 mol% (entry 4).



With the best conditions in hand, the researchers investigated the effects of substituents on the alkyne. A wide range of substituted alkynes were compatible with the reaction conditions and produced the correspondingly substituted isoindolinones **18–23** in moderate yields. Electron-donating methoxy-substituted alkynes reacted with **14** to afford **22** and its isomer **23** in 53% and 21% yields, respectively (Scheme 5b).

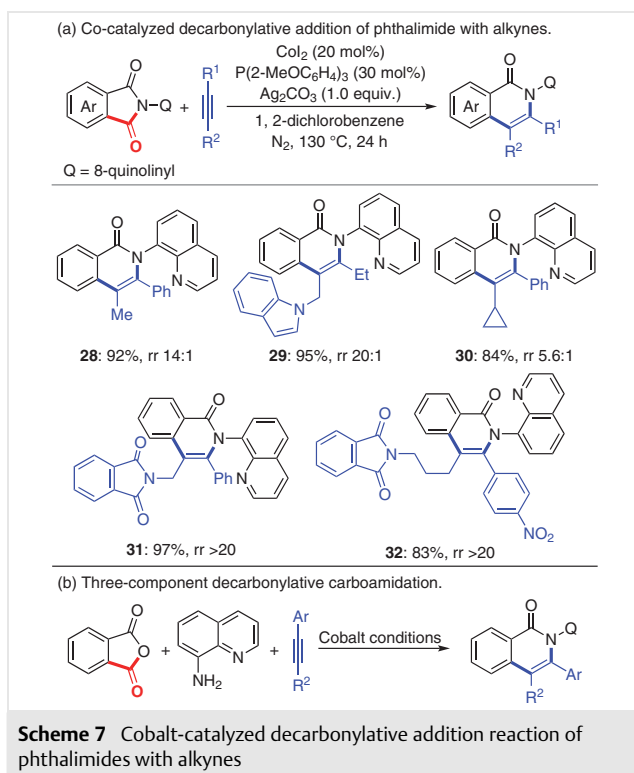
As shown in Scheme 6, the proposed mechanism began with the oxidative addition of an Ni(0) complex to an imide N–C(O) bond with the help of MAD. Subsequent decarbonylation, coordination, and isomerization gives cyclic cationic nickel complex **25**. The electron-rich phosphine ligands play very important roles in the stability of **25**. Nucleophilic addition of alkynes then takes place to afford cationic nickel disubstituted vinylidene intermediate **26** via a silyl group [1,2]-shift. Finally, reductive elimination furnishes the isoindolinone products and regenerates the initial Ni(0) catalyst. Notably, steric hindrance between the trimethylsilyl groups and the phosphine ligands on the nickel provides intermediate **27**, rather than **27'**.



## 2.2 Cobalt Catalysis

Despite advances in other transition-metal-catalyzed decarbonylations of amides,<sup>21</sup> including pioneering works with Ni, Ru, Pd, Rh, methods were still limited to the use of noble transition metals or unstable catalysts. In 2020, Chen and co-authors reported the first example of a cobalt-catalyzed decarbonylative addition reaction of phthalimide with alkynes (Scheme 7).<sup>22</sup> For cobalt-catalyzed imide decarbonylation, the P(2-MeOC<sub>6</sub>H<sub>4</sub>)<sub>3</sub> donating ligand and Ag<sub>2</sub>CO<sub>3</sub> oxidant were critical. Firstly, the electron-donating ligand promoted the oxidative addition of cobalt to the N–C(O) imide bond. Interestingly, Ag<sub>2</sub>CO<sub>3</sub> was essential for this reaction. A series of control experiments showed that coordinative CO could be oxidized by a silver ion and left as CO<sub>2</sub>. Under standard conditions, these reactions exhibited good regioselectivity when asymmetrical alkynes were used (**28–32**) (Scheme 7a). Selective decarbonylative annulations of phthalimide derivatives with phthalimide-substituted alkynes were compatible in these protocols, which provided isoquinolones (**31**, **32**) bearing phthalimide groups in high yields and regioselectivities (>20:1) (Scheme 7a). In addition, three-component decarbonylative addition reactions were accomplished by the use of phthalic anhydrides, 8-aminoquinolines, and alkynes (Scheme 7b). In comparison with traditional C–H activation strategies, the three-component reaction provided a more convenient and alternative scheme to access analogous cyclic products.

Interestingly, in the absence of alkynes, the decarbonylative homocoupling product **34** could be obtained in 35% yield. The addition of stoichiometric H<sub>2</sub>O prevented the formation of **34**. Next, to gain insight into the role of the oxidant, the gas phase of the reaction mixture was analyzed by

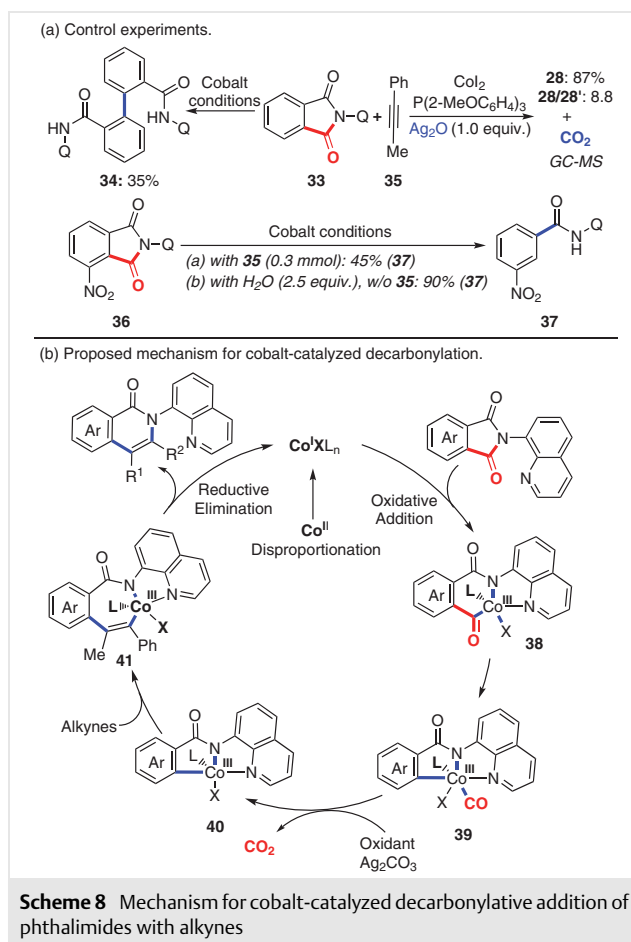


GC-MS with silver oxide added as the oxidant. Carbon dioxide was detected as the major gas component, which suggested that the silver oxide acted as a CO scavenger in the cobalt-catalyzed decarbonylation. The corresponding alkyne insertion and cyclization product was not detected when nitro-group-substituted **36** was treated under the standard conditions. Only decarbonylative product **37** was obtained in 45% yield. Product **37** could be obtained in 90% yield with external water as an additive (Scheme 8a).

A proposed cobalt catalytic cycle is depicted in Scheme 8b. Firstly, Co(II) undergoes disproportionation to form the active Co(I) species. By means of oxidative addition, Co(I) activates the C–N bond of the phthalimide to form Co(III) intermediate **38**. Subsequent decarbonylation leads to cobalt complex **39**. As a CO scavenger, external oxidant  $\text{Ag}_2\text{CO}_3$  facilitates the formation of active aryl-Co intermediate **40**. The alkyne undergoes coordination and migratory insertion to afford seven-membered cobaltacycle complex **41**. The final reductive elimination process produces the desired isoquinolone product and regenerates the Co(I) catalyst.

### 2.3 Rhodium Catalysis

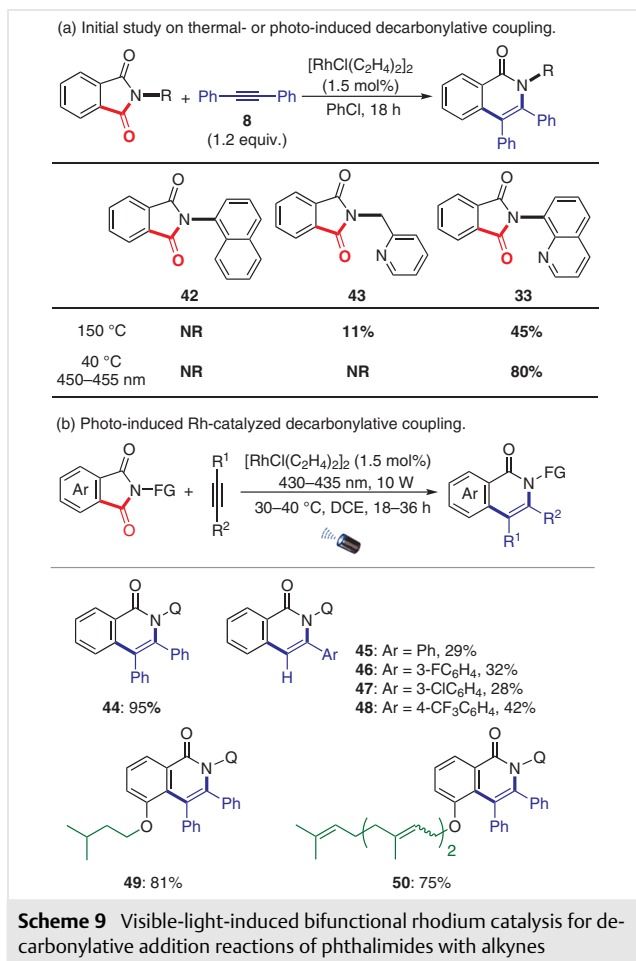
The pioneering work on  $\text{RhCl}(\text{PPh}_3)_3$  mediated decarbonylative reactions of aldehydes was done by Tsuji and Ohno.<sup>23</sup> In this reaction,  $\pi$ -backbonding between CO and Rh



impeded the ligand dissociation step to regenerate the Wilkinson's catalyst under mild conditions. To solve this problem, scientists were forced to adopt the thermal dissociation (usually at 110–200 °C) of CO from the resting state of the catalyst to facilitate catalytic regeneration. Therefore, it was of great interest to develop mild conditions for the catalytic decarbonylation.

In 2020, Chen and co-workers reported a Rh catalyzed decarbonylative addition reaction using visible light to promote the decarbonylation process (Scheme 9).<sup>18b</sup> An initial investigation suggested the functional group on the nitrogen atom of the imide played an important role in the reaction outcomes (Scheme 9a). Under thermal-induction conditions (150 °C), low yields (11–45%) could be obtained with pyridyl or quinolynyl as the functional group. Under photoinduced conditions (450–455 nm, 40 °C), a dramatic functional group effect was observed in that only the quinoline-substituted substrates delivered the expected cross-addition products in 80% yield. These initial results indicated that the functional group played a bifunctional role as a directing group and an energy-transfer promoter.

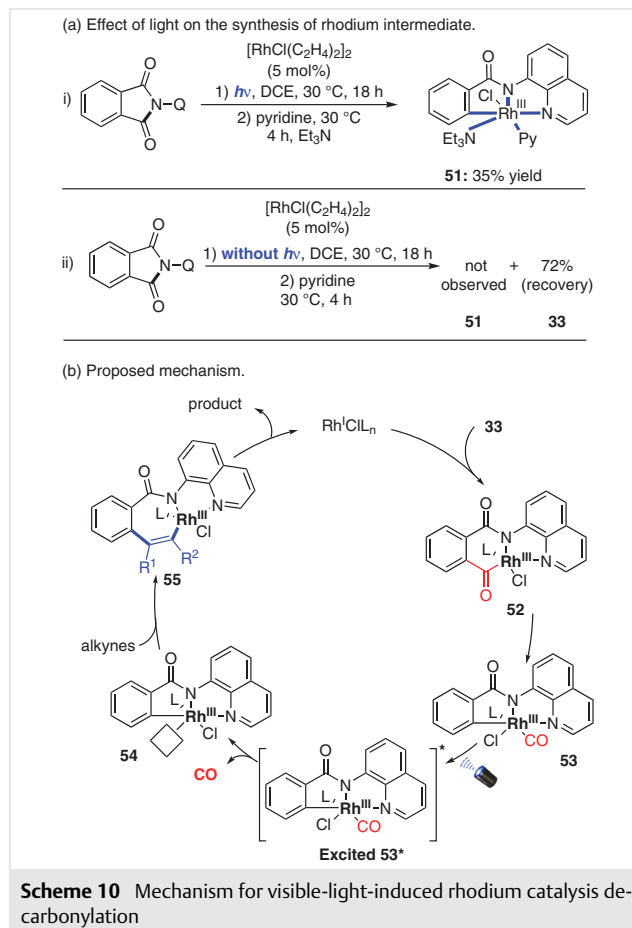




The generality of the alkyne and phthalimide substrates was subsequently investigated. A series of terminal alkynes could be well tolerated and delivered isoquinolones **45–48** in 28–42% yields, which were unusual because of the existence of a dominant [2+2+2] cycloaddition side reaction.<sup>24</sup> Furthermore, unsymmetrical phthalimides possessing a methoxy group on the 6-position of the quinoline ring successfully furnished the regiospecific products **49** and **50** in 75–81% yield, which constituted an important complement to the reported C–H activation strategies for 5-substituted isoquinolinone synthesis (Scheme 9b).

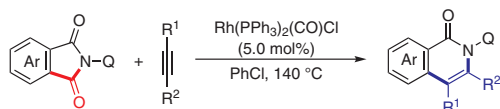
To elucidate the role of visible light, the researchers performed some control experiments (Scheme 10a). After light irradiation and subsequent purification, the reaction of [RhCl(C<sub>2</sub>H<sub>4</sub>)<sub>2</sub>]<sub>2</sub> with phthalimide slowly generated the unexpected saturated coordination complex **51** (18-electron). In the absence of visible light irradiation, no Rh complexes were formed and only phthalimide **33** was recovered in 72%. The UV/Vis absorption spectra of **51** showed a strong absorbance in the region of 390–420 nm. No desired product was observed in the absence of light. Under light irradiation, **44** was obtained in 95% yield. Overall, the above re-

sults suggest that the rhodium complex simultaneously served as the catalytic center and a photosensitizer for decarbonylation.



A plausible mechanism is depicted in Scheme 10b. The reaction is initiated from the oxidative addition of the Rh(I) species into the phthalimide C–N bond to form Rh(III) intermediate **52**. Subsequent deinsertion of carbon monoxide breaks the C–C bond to give Rh complex **53**. Under visible light irradiation, the excited state Rh complex **53\*** is generated, in which the transfer of an electron from the  $\pi$ -backbonding Rh–CO orbital into the antibonding orbital decreases the bond dissociation energy of the Rh–CO bond. This leads to subsequent CO extrusion under mild conditions to give the Rh intermediate **54** with a vacant coordination site. The coordination and migratory insertion of the alkyne delivered the seven-membered Rh complex **55**, which underwent reductive elimination to form the isoquinolone and regenerated the Rh(I) catalyst.

Notably, during the process of the Chen group's study,<sup>18b</sup> a thermally induced decarbonylative addition of imides with alkynes was reported by Xu *et al.*<sup>18a</sup> It should be noted that high temperature (140 °C) and a high catalyst loading (5 mol%) were essential for this reaction (Scheme 11).

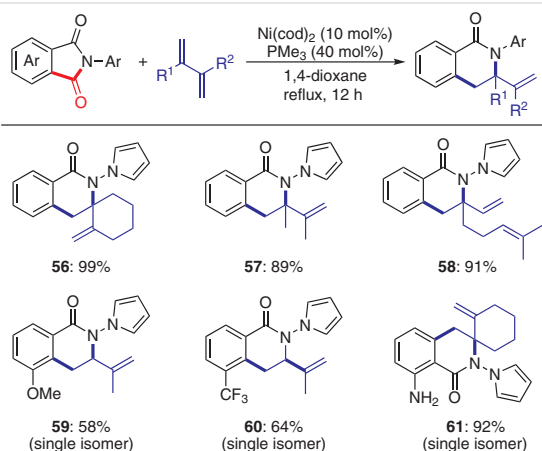


**Scheme 11** Thermal-induced decarbonylative addition reaction

### 3 Decarbonylative Addition Reaction with Alkenes

#### 3.1 Nickel Catalysis

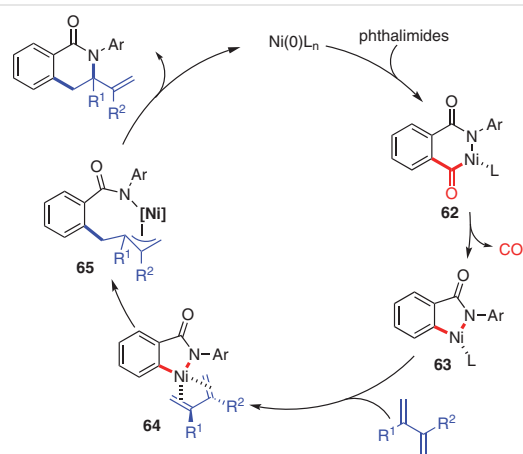
Similar to the Ni-catalyzed decarbonylative cycloaddition of phthalimides with alkynes, the Kurahashi and Matsubara group reported a decarbonylative cycloaddition of phthalimides with 1,3-dienes in 2010, which provided 3-vinyl-dihydroisoquinolones regioselectively.<sup>15</sup> The reaction presented an unprecedented replacement reaction of a carbon monoxide by a C–C single bond of a readily available heterocyclic compound (Scheme 12). In this reaction, screening of ligands showed that  $\text{PMe}_3$  gave the highest yield. Pyrrolyl as the *N*-substituent group gave a higher reaction yield than other groups.



**Scheme 12** Nickel-catalyzed decarbonylative cycloaddition of phthalimides with 1,3-dienes

The cycloaddition of phthalimides with symmetrical or unsymmetrical 1,3-dienes such as 1,2-dimethylenecyclohexane, 2,3-dimethyl-1,3-butadiene, and myrcene gave the 3-vinyl-dihydroisoquinolones in 89–99% yield. Notably, 3-methoxyphthalimide and 3-trifluoromethylphthalimide reacted regioselectively with isoprene to afford **59** and **60** as single isomers. Interestingly, the reaction of 3-aminophthalimide with isoprene could selectively provide **61** in 92% yield because of keto–enol tautomerism.

A plausible reaction pathway for this reaction is outlined in Scheme 13. The catalytic cycle is initiated from the oxidative addition of the CO–N bond to an Ni(0) complex to form nickel(II) intermediate **62**. Subsequent decarbonylation and coordination of the bidentate diene takes place to give Ni(II) intermediate **63**. The diene then inserts into the C–Ni bond to give the more stable acyclic  $\pi$ -allylnickel intermediate **64**. Nucleophilic addition of the nitrogen atom onto the  $\pi$ -allylnickel at the more substituted carbon atom takes place to afford **65**. The product is then released and the initial Ni(0) complex is regenerated.



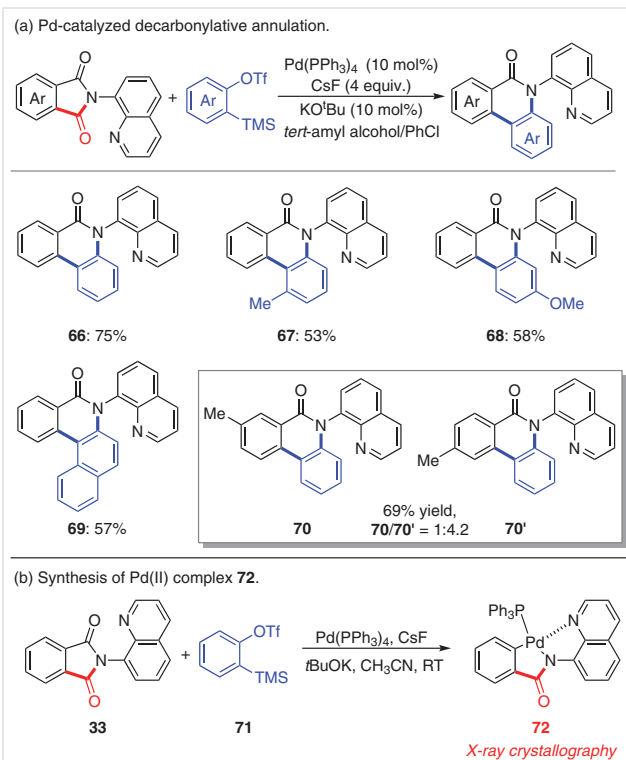
**Scheme 13** Mechanism for decarbonylative cycloaddition of phthalimides with 1,3-dienes

### 4 Decarbonylative Addition Reaction with Benzyne

#### 4.1 Palladium Catalysis

Inspired by the Ni(0)-catalyzed decarbonylative addition of phthalimides with alkynes, in situ formed arynes were chosen as addition partners. In 2019, Meng, Xu and co-workers reported the first palladium-catalyzed decarbonylative annulation reactions of phthalimides with arynes for the synthesis of phenanthridinones, which are widely present in various bioactive natural products and pharmaceuticals (Scheme 14a).<sup>17b</sup>

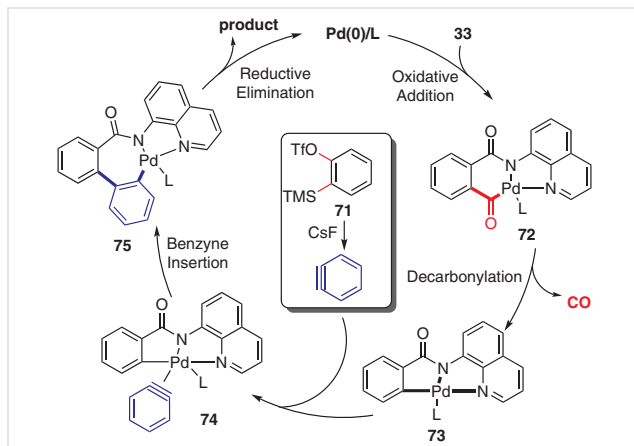
The reactions gave moderate to high yields under the optimized conditions. Both electron-donating and electron-withdrawing groups were tolerated with phthalimides and arynes. However, the optimized conditions could not control the regioselectivity satisfactorily when unsymmetric phthalimides or aryne precursors were used as substrates (e.g., **70** and **70'**) (Scheme 14a).



**Scheme 14** Palladium-catalyzed decarbonylative annulation of phthalimides with arynes

To gain insight into the reaction mechanism, the reaction of  $\text{Pd}(\text{PPh}_3)_4$  with phthalimides and Kobayashi benzyne precursor **71** was performed. As expected, the stable Pd(II) complex **72** was formed, for which the structure and relative stereochemistry were rigorously confirmed by X-ray crystallography (Scheme 14b).

Based on the X-ray crystallography result of intermediate **72** and previous research reported by the Matsubara and Kurahashi group,<sup>14</sup> a plausible mechanism was pro-



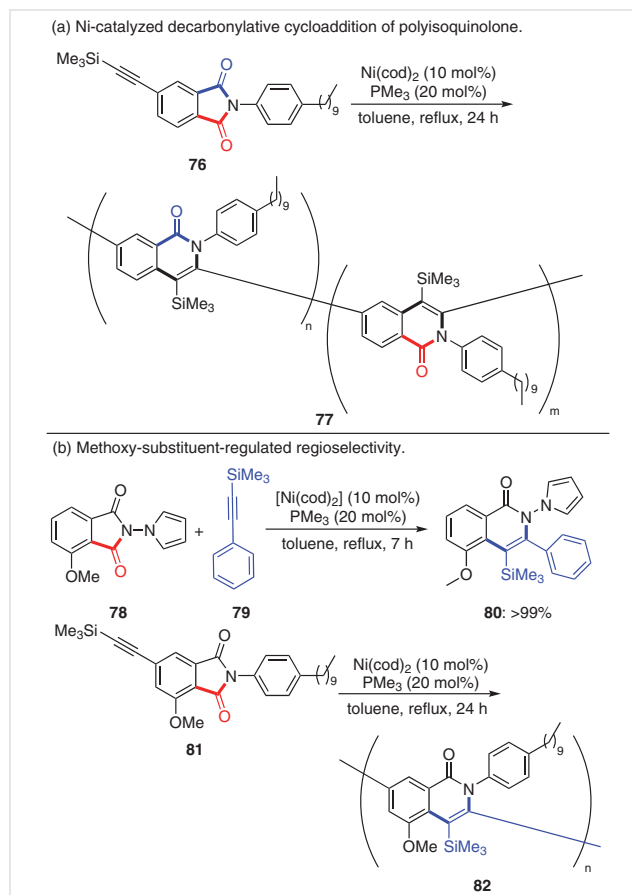
**Scheme 15** Proposed mechanism for palladium-catalyzed decarbonylative annulation of phthalimides with arynes

posed and is shown in Scheme 15. The decarbonylative process is similar to the pathways mentioned in previous research. Elimination of the TMS and OTf groups in **71** generates an active benzyne species, which undergoes insertion of the C–C triple bond into the Pd–aryl complex. A final reductive elimination of **75** leads to the product.

## 5 Decarbonylative Polymerization

### 5.1 Nickel Catalysis

Decarbonylative annulations of phthalimides with alkynes could also be applied as an elementary step for polymerization. In 2012, Takeuchi *et al.* managed to synthesis polyisoquinolones by using alkynyl-substituted phthalimides as original monomers (Scheme 16).<sup>25</sup> A methoxy moiety was introduced at the *ortho* position of the amide to serve as a directing group in regioselective oxidative addition of Ni(0). Single monomer products of polyisoquinolones were successfully obtained by using this strategy (Scheme 16b).



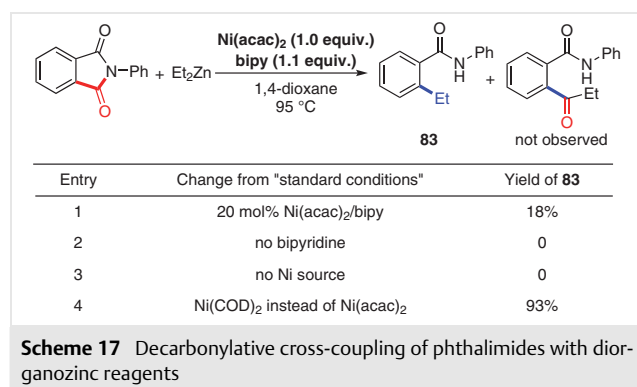
**Scheme 16** Nickel-catalyzed decarbonylative polymerization of 5-alkynylphthalimides



## 6 Decarbonylative Alkylation

### 6.1 Nickel Catalysis

In 2011, Johnson and co-workers discovered that nickel-mediated cross-coupling of phthalimides with diorganozinc reagents could proceed via a decarbonylative process to produce *ortho*-alkyl-substituted benzamides (Scheme 17).<sup>26</sup> Significantly, the yields of these reactions were closely matched to the nickel loading, suggesting a failure of nickel catalytic turnover. No desired products were observed when the reactions were performed in the absence of ligands or nickel catalysis (entries 2 and 3). In addition, Ni(COD)<sub>2</sub> also proved to be a viable metal source for the reaction (entry 4).

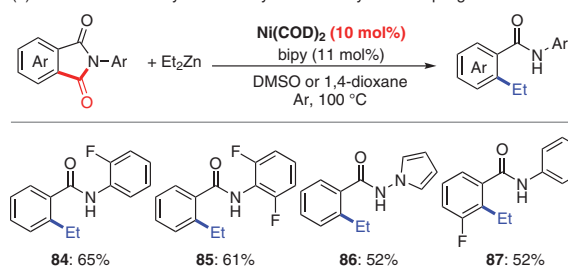


Furthermore, the ketamide product anticipated from direct coupling of the imide and diethylzinc was not observed. It was presumed that an Ni–CO complex was formed after one catalytic cycle, which indicated that the strong Ni–CO bond prevented regeneration of the Ni(0) species.

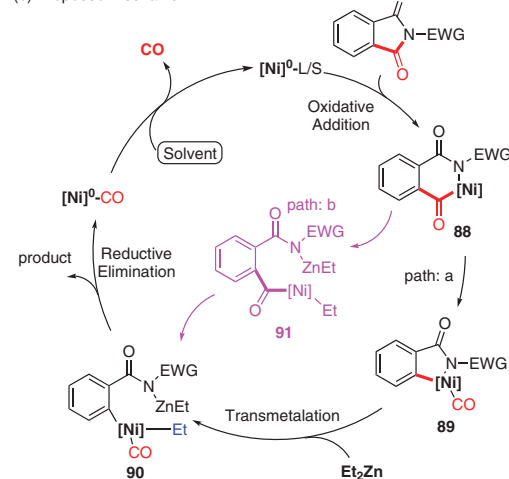
To circumvent this problem, the authors tried using various  $\pi$ -accepting ligands combined with different solvents. However, none of the conditions led to the expected decarbonylative coupling products. Based on previous studies about the influences of *N*-protecting groups, the authors chose electron-withdrawing groups on *N*-substituents (**84–87**), which enabled the reaction to proceed with a catalytic amount of nickel catalysis (Scheme 18a).<sup>27</sup> The results indicated that CO dissociation was prior to *N* dissociation from the metal center. Apart from electron-withdrawing *N*-protecting groups, electron-deficient *ortho* substituents would also facilitate the catalytic process and only a single regioisomer was formed when *o*-fluorinated phthalimide was used as the substrate.

The proposed mechanism is presented in Scheme 18b. Firstly, the active Ni(0) complex undergoes oxidative addition to generate metallacycle intermediate **88**, which undergoes decarbonylation and transmetalation to generate complex **90**. Reductive elimination and acid workup give

(a) Efforts toward catalysis for catalytic decarbonylative coupling.



(b) Proposed mechanism.



**Scheme 18** Decarbonylative cross-coupling of phthalimides with diorganozinc reagents

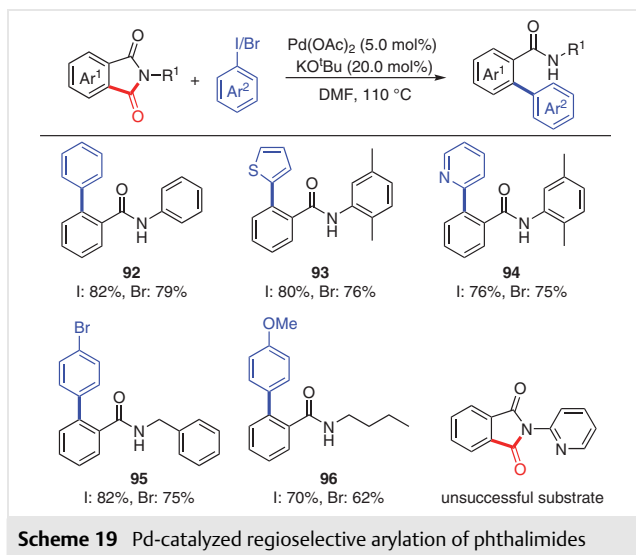
the *ortho*-substituted benzamides and regenerated Ni–CO complex. In a potential alternative, **88** could undergo transmetalation prior to decarbonylation, which would generate complex **91**.

## 7 Decarbonylative Arylation

### 7.1 Palladium Catalysis

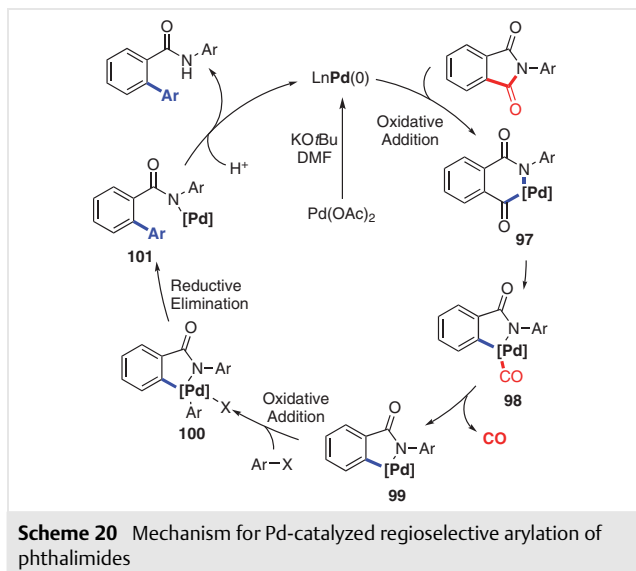
In 2019, Samanta and Biswas reported the Pd-catalyzed decarbonylative arylation of phthalimide with aryl halides (Scheme 19).<sup>17a</sup> No ligands were required for this transformation. On the contrary, introduction of a ligand into the system led to decreased yields. The base and solvent had a significant impact on the reactivity, because they could participate in the regeneration of the catalytically active Pd(0) species.

A wide range of substituted phenyl and heterocyclic halides were well tolerated in this system, and the reactivity of aryl iodide was slightly better than aryl bromide (Scheme 19). A sterically demanding aryl *N*-protecting group was also tolerated. However, an *N*-protecting group



containing a strong coordinating atom inhibited the reaction by forming a stable Pd(II) complex.

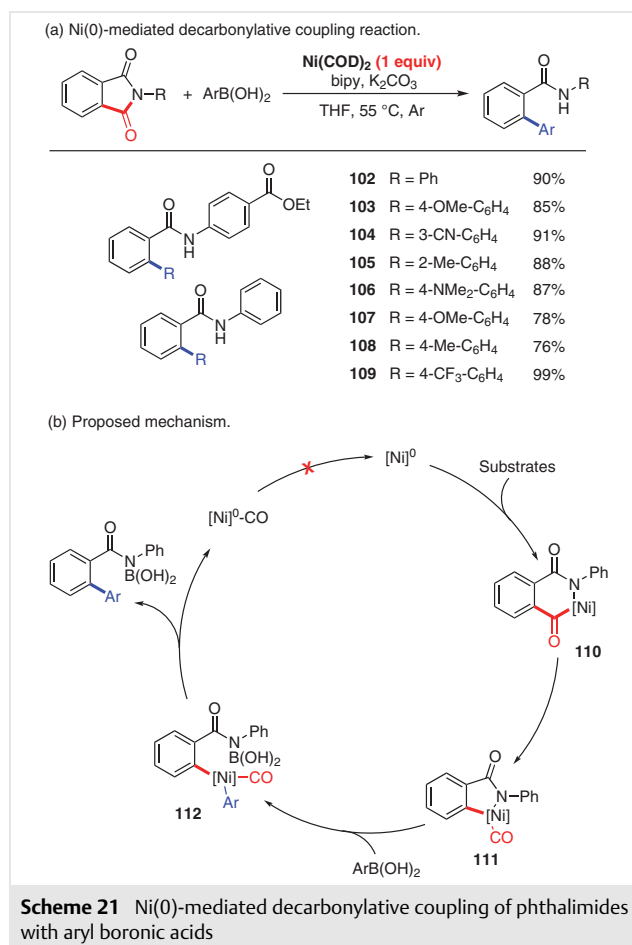
Based on several control experiments, the authors proposed a mechanism (Scheme 20). Firstly, Pd(II) is reduced to Pd(0) by DMF and base. The Pd(0) species is then inserted into the amide C–N bond by oxidative addition. After thermal decarbonylation, the aryl halide reacts with Pd(II) species **99** via oxidative addition to generate Pd(IV) species **100**. The product is obtained from intermediate **101** and the Pd(0) is regenerated in the presence of DMF.



## 7.2 Nickel Catalysis

In 2020, Johnson and co-workers reported Ni(0)-mediated decarbonylative coupling of phthalimide with aryl boronic acid.<sup>28</sup> Relative to diorganozinc as the transmetalation reagent, aryl boronic acid was more compatible with active

groups such as ketones and esters (Scheme 21). In addition, the steric effect of aryl boronic acid had almost no effect on the reactivity. The proposed mechanism was similar to that of the Ni-catalyzed alkylation reported by the same group in 2016.<sup>27</sup> However, similar to their previous report in 2011,<sup>26</sup> this reaction required a stoichiometric amount of Ni(0), which might indicate that the strong binding force of Ni–CO inhibited the catalytic cycle. Introduction of electron-withdrawing groups to the N atom of the phthalimide also failed to facilitate dissociation of the CO ligand.

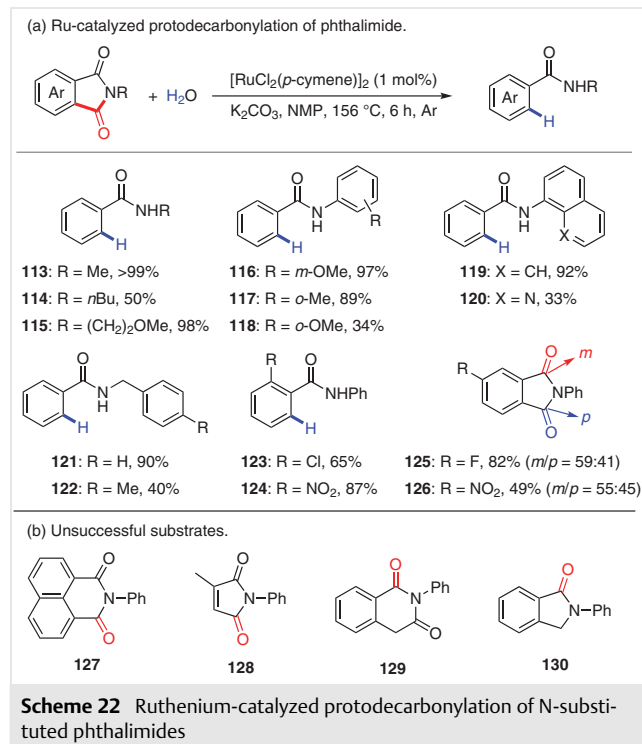


## 8 Protodecarbonylation

### 8.1 Ruthenium Catalysis

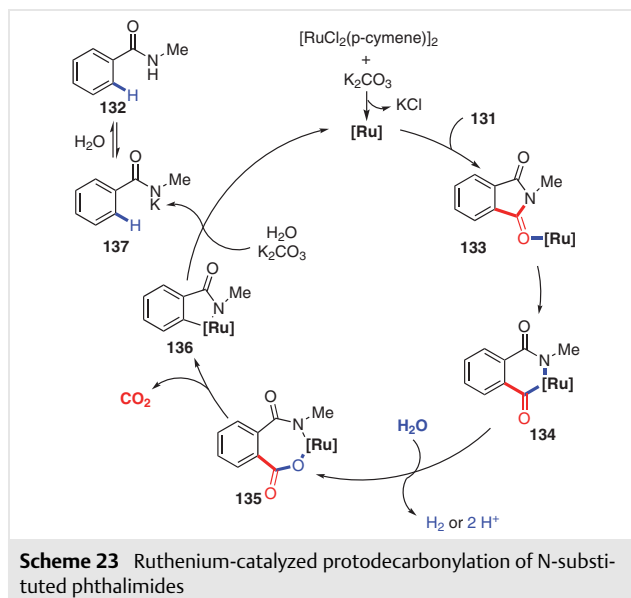
In 2020, Gramage-Doria and co-workers reported an unexpected protodecarbonylation of phthalimides into amides.<sup>29</sup> These Ru-catalyzed decarbonylative transformations were achieved in high yields and short reaction times (**113**–**124**). However, satisfactory results were not achieved with selective decarbonylation of phthalimide substituted with aromatic rings (**125** and **126**) (Scheme 22a). Notably, the reaction with the six-membered-ring phthalimide **127** did

not proceed under standard conditions, indicating that the ring strain released in the six-membered-ring phthalimide was probably the driving force for the initial step of the catalytic cycle. Furthermore, substrates **128–130** bore structural resemblance to phthalimides that did not react in the protodecarbonylation reaction (Scheme 22b).



To gain insight into the reaction mechanism, the gas phase of the reaction mixture was analyzed by GC. Differently from the traditional decarbonylation reaction mechanism, CO was not formed in this system. Instead, H<sub>2</sub> and CO<sub>2</sub> were detected by GC. The reaction only gave 8% yield of product when 1 bar of H<sub>2</sub> was introduced into the system, which indicated that H<sub>2</sub> did not participate in the catalytic cycle. Full incorporation of deuterium at the *ortho* position of the product suggested that H<sub>2</sub>O was the proton source. Interestingly, the reaction without H<sub>2</sub>O also achieved 56% yield. The authors argued that a trace amount of water in K<sub>2</sub>CO<sub>3</sub> might still serve as a proton source and the use of overnight-dried K<sub>2</sub>CO<sub>3</sub> powder led to a slightly decreased yield, which supported this opinion to a certain extent.

A mechanism is tentatively postulated in Scheme 23. Firstly, a ruthenium chloride free species is formed after the reaction of [RuCl<sub>2</sub>(*p*-cymene)]<sub>2</sub> with K<sub>2</sub>CO<sub>3</sub>. N- or O-coordination of the Ru species to **131** led to **133** or isomers. After ring opening, **134** was formed. Hydroxylation followed by release of a proton or hydrogen leads to **135**. After decarboxylation, ruthenacycle complex **136** was formed. Finally, **137** was obtained after protonolysis of **136**, and the Ru catalyst was regenerated.



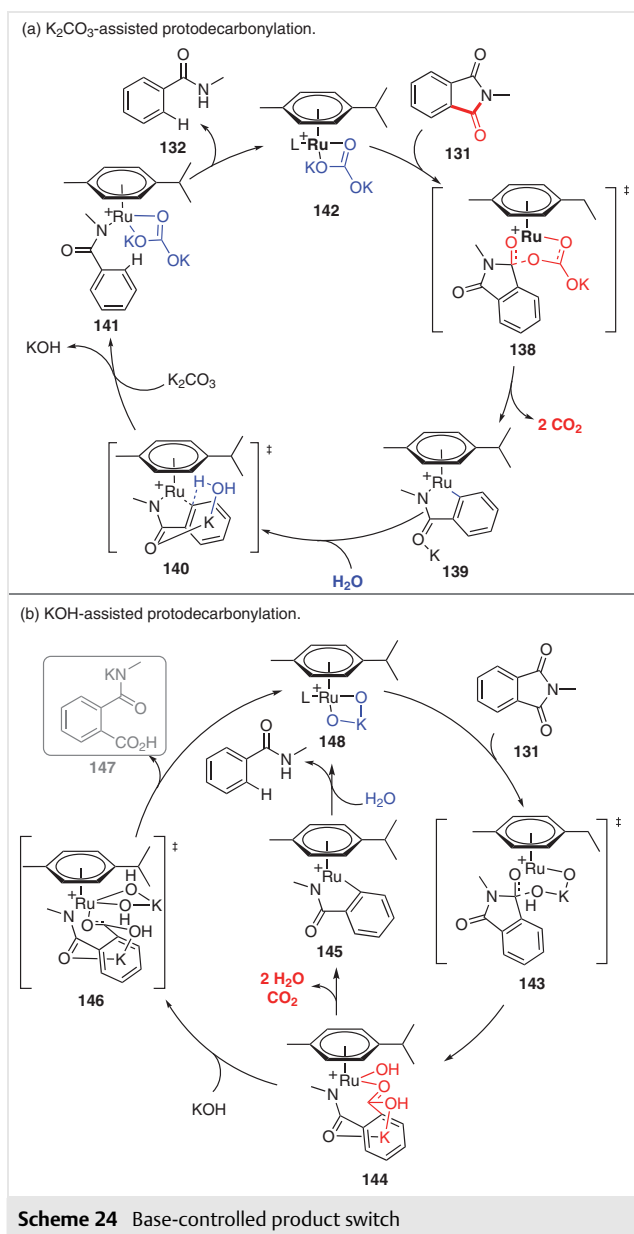
Later, the authors discovered that using KOH instead of K<sub>2</sub>CO<sub>3</sub> led to the formation of the hydrolysis product. DFT calculations were applied to explain this phenomenon (Scheme 24).<sup>30</sup> However, according to the DFT results, CO<sub>2</sub> was generated by K<sub>2</sub>CO<sub>3</sub>, which seemed to contradict the role of H<sub>2</sub>O as the source of H<sub>2</sub> proposed in their previous report.

Ruthenium-catalyzed protodecarbonylation of phthalimide derivatives into secondary amides needed to release two molecules of CO<sub>2</sub>. One came from the carbonyl group of the substrate, and the other came from K<sub>2</sub>CO<sub>3</sub>. Moreover, the potassium cations were relevant for stabilizing all of the intermediates via weak interactions. When the base additive was switched to KOH, high temperature led to the formation of secondary amides, and low temperature yielded the phthalamic acid derivative products. Interestingly, it was found that the ruthenium center exhibited an oxidation state of +2 through the whole catalytic cycle.

Phthalimides, and *N*-aryl phthalimides in particular, are prone to hydrolysis followed by decarboxylative coupling. Some examples discussed likely involve hydrolysis or a decarboxylative coupling mechanism. In terms of the net transformation, this is a protodecarbonylation process.

## 9 Conclusion and Outlook

To conclude, transition-metal-catalyzed decarbonylative reactions of phthalimides have exhibited unique and diverse chemical reactivities over the past decades. Initially, Matsubara group reported the first example of nickel-catalyzed decarbonylative addition of phthalimides to alkynes. In recent years, decarbonylative processes with other transition-metal catalysts, including Rh, Pd, Ru, and Co catalysts



have been developed by different groups. These feasible decarbonylative processes include decarbonylative addition reactions with alkynes, alkenes, and benzynes, protodecarbonylation, decarbonylative alkylation, and arylation schemes. Their utilities have been highlighted in the synthesis of some certain products.

Despite the remarkable progress, several challenges still need to be addressed. (1) In most cases, the reactions require relatively harsh conditions ( $>130\text{ }^\circ\text{C}$ ) and high catalyst loading. Although our group developed a photo-induced Rh-catalyzed decarbonylative addition reaction of phthalimides with alkynes, decarbonylative reactions of phthalimides with other units under mild conditions remain undeveloped. (2) The developed catalytic systems re-

quire electron-withdrawing *N*-protecting groups or directing groups on the phthalimides. The innovative designs of more efficient catalyst systems to solve these limitations continue to be important issues in this area.

Although studies of the transition-metal-catalyzed decarbonylative reactions of phthalimides have been described, the synthetic application of these protocols is still in its infancy and needs profound explorations. Phthalimides can also react with other unsaturated congeners, such as allenes, cyanides, isocyanides, and azide compounds. Their chemo- and regioselectivities need careful regulation as well. This Short Review is intended to be a foundation for the further developments of novel strategies to achieve decarbonylative derivatizations by using mild and sustainable conditions.

## Conflict of Interest

The authors declare no conflict of interest.

## Funding Information

Financial support from the National Natural Science Foundation of China (Grant Nos. 21971234, 21772194, and 21572225) is acknowledged.

## References

- (1) (a) Hideshima, T.; Chauhan, D.; Shima, Y.; Noopur, R.; Davies, F. E.; Tai, Y. T.; Treon, S. P.; Lin, B. K.; Schlossman, R. L.; Richardson, P. G.; Gupta, D.; Muller, G. W.; Stirling, D. I.; Anderson, K. C. *Blood* **2000**, *96*, 304A. (b) Tsunoda, T.; Yamazaki, A.; Iwamoto, H.; Sakamoto, S. *Org. Process Res. Dev.* **2003**, *7*, 883. (c) Ramirez-Flores, P. N.; Barraza-Reyna, P. J.; Aguirre-Vazquez, A.; Camacho-Moll, M. E.; Guerrero-Beltran, C. E.; Resendez-Perez, D.; Gonzalez-Villasana, V.; Garza-Gonzalez, J. N.; Silva-Ramirez, B.; Castorena-Torres, F.; Bermudez de Leon, M. *Molecules* **2021**, *26*, 5742. (d) Wang, D.; Wang, Y.; Sun, S. *Ren. Fail.* **2021**, *43*, 1425. (e) Zheng, W.; Fu, L. *Am. J. Transl. Res.* **2021**, *13*, 10809.
- (2) (a) Chapman, R. E.; Rigby, R. D. G. *Aust. J. Biol. Sci.* **1980**, *33*, 183. (b) Il'in, A. V.; Gubaev, A. F.; Islamov, D. R.; Islamov, K. R.; Galkin, V. I. *Chem. Heterocycl. Compd.* **2021**, *57*, 175.
- (3) (a) Keating, G. M. *Drugs* **2017**, *77*, 459. (b) Deeks, E. D. *Drugs* **2020**, *80*, 181.
- (4) (a) Scott, L. J. *Drugs* **2014**, *74*, 549. (b) Hartmann, M. D.; Boichenko, I.; Coles, M.; Zanini, F.; Lupas, A. N.; Alvarez, B. H. *J. Struct. Biol.* **2014**, *188*, 225.
- (5) (a) Isoherranen, N.; Yagen, B.; Spiegelstein, O.; Finnell, R. H.; Merriweather, M.; Woodhead, J. H.; Wlodarczyk, B.; White, H. S.; Bialer, M. *Br. J. Pharmacol.* **2003**, *139*, 755. (b) Gupta, R. C.; Win, T.; Bittner, S. *Curr. Med. Chem.* **2005**, *12*, 2021.
- (6) (a) Molina, E.; Diaz, H. G.; Gonzalez, M. P.; Rodriguez, E.; Uriarte, E. *J. Chem. Inf. Comput. Sci.* **2004**, *44*, 515. (b) Yosefdad, S.; Valadbeigi, Y.; Bayat, M. *J. Mol. Struct.* **2020**, *1200*, 127105.
- (7) (a) Hall, I. H.; Wong, O. T.; Scovill, J. P. *Biomed. Pharmacother.* **1995**, *49*, 251. (b) Lee, N.-J.; Jeong, I.-C.; Cho, M.-Y.; Jeon, C.-W.; Yun, B.-C. Y.; Kim, Y.-O.; Kim, S.-H.; Chung, I. *Eur. Polym. J.* **2006**, *42*, 3352. (c) Kok, S. H. L.; Gambari, R.; Chui, C. H.; Yuen, C. W.

- M.; Lin, E.; Wong, R. S. M.; Lau, F. Y.; Cheng, G. Y. M.; Lam, W. S.; Chan, S. H.; Lam, K. H.; Cheng, C. H.; Lai, P. B. S.; Yu, M. W. Y.; Cheung, F.; Tang, J. C. O.; Chan, A. S. C. *Biorg. Med. Chem.* **2008**, *16*, 3626. (d) Belluti, S.; Orteca, G.; Semeghini, V.; Rigillo, G.; Parenti, F.; Ferrari, E.; Imbriano, C. *Int. J. Mol. Sci.* **2019**, *20*, 28. (e) Philoppes, J. N.; Lamie, P. F. *Bioorg. Chem.* **2019**, *89*, 102978.
- (8) (a) Wang, Z.; Zhang, Y.; Zhang, H.; Harrington, P. B.; Chen, H. *J. Am. Soc. Mass. Spectrom.* **2012**, *23*, 520. (b) Kushwaha, N.; Kaushik, D. *J. Appl. Pharm. Sci.* **2016**, *6*, 60330, DOI: 10.7324/japs.2016.60330. (c) Quinn, R. K.; Koenst, Z. A.; Michalak, S. E.; Schmidt, Y.; Szklarski, A. R.; Flores, A. R.; Nam, S.; Horne, D. A.; Vanderwal, C. D.; Alexanian, E. J. *J. Am. Chem. Soc.* **2016**, *138*, 696. (d) Milan, M.; Carboni, G.; Salamone, M.; Costas, M.; Bietti, M. *ACS Catal.* **2017**, *7*, 5903. (e) Barsu, N.; Kalsi, D.; Sundararaju, B. *Catal. Sci. Technol.* **2018**, *8*, 5963.
- (9) (a) Hu, J.; Zhao, Y.; Liu, J.; Zhang, Y.; Shi, Z. *Angew. Chem. Int. Ed.* **2016**, *55*, 8718. (b) Malins, L. R. *Curr. Opin. Chem. Biol.* **2018**, *46*, 25. (c) Mangubat-Medina, A. E.; Martin, S. C.; Hanaya, K.; Ball, Z. T. *J. Am. Chem. Soc.* **2018**, *140*, 8401. (d) Willis, M. C.; McNally, S. J.; Beswick, P. J. *Angew. Chem. Int. Ed.* **2004**, *43*, 340.
- (10) (a) Rahman, M. M.; Buchspies, J.; Szostak, M. *Catalysts* **2019**, *9*, 129. (b) Li, G. C.; Ma, S. Y.; Szostak, M. *Trends Chem.* **2020**, *2*, 914. (c) Meng, G. R.; Zhang, J.; Szostak, M. *Chem. Rev.* **2021**, *121*, 12746.
- (11) García-Cárceles, J.; Bahou, K. A.; Bower, J. F. *ACS Catal.* **2020**, *10*, 12738.
- (12) (a) Hughes, A. K.; Wade, K. *Coord. Chem. Rev.* **2000**, *197*, 191. (b) Dobson, G. R. *Inorg. Chem.* **1980**, *19*, 1413.
- (13) (a) Stephan, M. S.; Teunissen, A.; Verzijl, G. K. M.; de Vries, J. G. *Angew. Chem. Int. Ed.* **1998**, *37*, 662. (b) Goossen, L. J.; Ghosh, K. *Angew. Chem. Int. Ed.* **2001**, *40*, 3458.
- (14) Kajita, Y.; Matsubara, S.; Kurahashi, T. *J. Am. Chem. Soc.* **2008**, *130*, 6058.
- (15) Fujiwara, K.; Kurahashi, T.; Matsubara, S. *Org. Lett.* **2010**, *12*, 4548.
- (16) Shiba, T.; Kurahashi, T.; Matsubara, S. *J. Am. Chem. Soc.* **2013**, *135*, 13636.
- (17) (a) Samanta, P. K.; Biswas, P. J. *Org. Chem.* **2019**, *84*, 3968. (b) Meng, Y. Y.; Si, X. J.; Song, Y. Y.; Zhou, H. M.; Xu, F. *Chem. Commun.* **2019**, 55, 9507. (c) Li, C.; Li, P.; Yang, J.; Wang, L. *Chem. Commun.* **2012**, 48, 4214.
- (18) (a) Xu, F.; Zhu, W. J.; Wang, J.; Ma, Q.; Shen, L. J. *Org. Biomol. Chem.* **2020**, *18*, 8219. (b) Min, X. T.; Ji, D. W.; Guan, Y. Q.; Guo, S. Y.; Hu, Y. C.; Wan, B.; Chen, Q. A. *Angew. Chem. Int. Ed.* **2021**, *60*, 1583. (c) Zeng, R.; Chen, P.-h.; Dong, G. *ACS Catal.* **2016**, *6*, 969.
- (19) (a) Grigorjeva, L.; Daugulis, O. *Org. Lett.* **2014**, *16*, 4688. (b) Fu, L.-Y.; Ying, J.; Wu, X.-F. *J. Org. Chem.* **2019**, *84*, 12648. (c) Gruener, B.; Sicha, V.; Hnyk, D.; Londesborough, M. G. S.; Cisarova, I. *Inorg. Chem.* **2015**, *54*, 3148. (d) Tonigold, M.; Lu, Y.; Mavrandonakis, A.; Puls, A.; Staudt, R.; Moellmer, J.; Sauer, J.; Volkmer, D. *Chem. Eur. J.* **2011**, *17*, 8671. (e) Cabrero-Antonino, J. R.; Adam, R.; Papa, V.; Holsten, M.; Junge, K.; Beller, M. *Chem. Sci.* **2017**, *8*, 5536.
- (20) (a) Zheng, C.; Wang, Y.; Xu, Y.; Chen, Z.; Chen, G.; Liang, S. H. *Org. Lett.* **2018**, *20*, 4824. (b) Hu, A. G.; Lin, W. B. *Org. Lett.* **2005**, *7*, 455.
- (21) Liu, C.; Szostak, M. *Org. Biomol. Chem.* **2018**, *16*, 7998.
- (22) Min, X. T.; Ji, D. W.; Zheng, H.; Chen, B. Z.; Hu, Y. C.; Wan, B.; Chen, Q. A. *Org. Lett.* **2020**, *22*, 3386.
- (23) Tsuji, J.; Ohno, K. *Tetrahedron Lett.* **1965**, *44*, 3969.
- (24) (a) Wang, C.; Li, X.; Wu, F.; Wan, B. *Angew. Chem. Int. Ed.* **2011**, *50*, 7162. (b) Neumeier, M.; Chakraborty, U.; Schaarschmidt, D.; de la Pena O'Shea, V.; Perez-Ruiz, R.; Jacobi von Wangelin, A. *Angew. Chem. Int. Ed.* **2020**, *59*, 13473.
- (25) Takeuchi, M.; Kurahashi, T.; Matsubara, S. *Chem. Lett.* **2012**, *41*, 1566.
- (26) Havlik, S. E.; Simmons, J. M.; Winton, V. J.; Johnson, J. B. *J. Org. Chem.* **2011**, *76*, 3588.
- (27) DeGlopper, K. S.; Fodor, S. K.; Endean, T. B. D.; Johnson, J. B. *Polyhedron* **2016**, *114*, 393.
- (28) Heyboer, E. M.; Johnson, R. L.; Kwiatkowski, M. R.; Pankratz, T. C.; Yoder, M. C.; DeGlopper, K. S.; Ahlgrim, G. C.; Dennis, J. M.; Johnson, J. B. *J. Org. Chem.* **2020**, *85*, 3757.
- (29) Yuan, Y. C.; Kamaraj, R.; Bruneau, C.; Labasque, T.; Roisnel, T.; Gramage-Doria, R. *Org. Lett.* **2017**, *19*, 6404.
- (30) D'Alterio, M. C.; Yuan, Y.-C.; Bruneau, C.; Talarico, G.; Gramage-Doria, R.; Poater, A. *Catal. Sci. Technol.* **2020**, *10*, 180.